

Relations between electron beam welding parameters and appearances of weld beads on Nb plates

Takayuki Kubo^{*A)}, Yasuo Ajima^{A)}, Tomohiro Nagata^{B)}, Takayuki Saeki^{A)},
Kensei Umemori^{A)}, Yuichi Watanabe^{A)},

^{A)}High energy accelerator research organization, KEK,
1-1 Oho, Tsukuba, Ibaraki 305-0801 Japan

^{B)}ULVAC, Inc., 5-9-6 Tokodai, Tsukuba, Ibaraki 300-2635 Japan

Abstract

We studied relations between electron beam welding parameters and appearances of weld beads. Allowed parameter regions to obtain a full penetration weld without hole or spattering, a relation between underbead width and EBW parameters, and a relation among a peak height, valley depth and underbead width were also examined. We found that a beam generator direction and beam sweep direction affect a geometry of weld bead dramatically, a focused beam cause a wide underbead, a peak height is proportional to underbead width for the vertical generator position, and neither a peak height nor valley depth shows a simple linearity as a function of underbead width for the horizontal generator position with horizontal beam sweep.

INTRODUCTION

Surface defects of superconducting rf (SRF) cavity cause locally enhanced electric and magnetic field, and trigger electron field emissions and thermal magnetic break down [1]. Therefore surfaces must be smooth. On and around electron beam welding (EBW) seams, however, defects are often found [2]. An optimum parameter of EBW to minimize a number of defects should be studied.

One approach to the above problem is analyzing sample Nb plates with weld beads. Fortunately, we have an environment necessary for preparing these sample plates [3, 4]. An EBW machine installed in KEK cavity fabrication facility (CFF), where machines needed to make cavities are all equipped in one clean environment, can be used to prepare weld beads on pure Nb plates right after buffered chemical polishing (BCP). As a first step of this approach, we studied relations between parameters of EBW machine and appearances of weld beads.

EXPERIMENT

By a EBW parameter, we mean accelerating voltage V_a , beam current I_b , sweep speed v , focus current I_f and direction of the beam generator. Note that $V_a I_b$ is a input beam power. v determines a input power per unit length through $V_a I_b / v$. I_f is a current on the focus coil to adjust focal length and determines a power density on the surface of

work piece for a fixed V_a and I_b . A generator position determines a direction of target Nb coupon, namely, a relative direction of gravity acting on molten Nb. These five parameters all affect an appearance of weld bead.

Focusing effect of focus current

It is important to note that a focusing effect of a specific value of focus current varies greatly depending on an accelerating voltage. For a different V_a , a different I_f is needed in order to collect an electron beam to the same distance L from a tip of electron beam gun. Namely, I_f is a function of V_a and L . In other words, a distance L , to which an electron beam is collected, is given by a function of V_a and I_f . For analysing relations between EBW parameters and appearances of weld beads from a unified view point, we need to examine a relation among V_a , I_f and L .

Since we do not know the inside of our machine (Steigerwald Strahltechnik EBOCAM KS110-G150 KM-CNC), we regard the machine as a black box and analyse a relation between inputs and outputs. Here inputs means V_a and L , and outputs means I_f which realize a beam spot with the highest power density for fixed V_a and L . In the following we call such a focus current a just focus current I_f^0 . The experimental procedure is as follows:

1. Search a just focus current I_f^0 which realize a beam spot with the highest power density for a fixed V_a and L . A just focus current is found by watching a shine from a beam spot as it radiates the brightest light.
2. Increase L by 100 mm and repeat 1.
3. Increase V_a by 30 kV and repeat 1 and 2.

In the next section, we will analyse the results and obtain a formula combining V_a , I_f^0 and L . The formula will be used to analyse results from experiment in the following.

Analyse coupons with weld beads

We prepared a number of Nb coupons with size of 150 mm \times 150 mm \times 2 mm which were cut from cavity-grade Nb sheet. Pre-weld etching was applied to these coupons at CFF, where 10 – 30 μ m of materials were removed by using BCP solution which consist of 85% phosphoric acid, 67% nitric acid and 46% hydrofluoric acid with

* kubitaka@post.kek.jp

Table 1: EBW parameters for Nb sample test

Generator Position	vertical or horizontal
Sweep Speed v	3 or 5 mm/s
Accelerating Voltage V_a	60, 90, 120 or 150 kV
Beam Current I_b	10 - 40 mA
Focus Current I_f	1000 - 3000 mA

the ratio of 1:1:1. Following ultrapure water rinsing, etched coupons were carried to the next room in CFF in which the EBW machine were installed. We then formed a number of weld beads on coupons by varying the parameters of the EBW machine, namely, V_a , I_b , v , I_f and generator position as shown in Table 1. Totally, we obtained a few hundred weld beads.

We examined appearance of weld beads. Existence or absence of holes and spattering, and smoothness of weld beads were checked. In addition, we measured widths, heights and depths of underbeads by using a surface profiler (Veeco Dektak 150) in ULVAC tsukuba institute which can measure surface profile with 0.1 nm, 1 nm and 8 nm vertical resolution for the measurement range of $6.5 \mu\text{m}$, $65.5 \mu\text{m}$ and $524 \mu\text{m}$, respectively. Note that the underbead is the melted zone on the side of the Nb coupon opposite the side where the electron beam is incident. Since the underbead corresponds to a weld bead on an inner surface of SRF cavity, examining its smoothness and geometry is essential to understanding optimum parameter of EBW.

RESULTS AND DISCUSSION

In the following, we first mention the results from an experiment to obtain a relation among accelerating voltage V_a , just focus current I_f^0 which realize a beam spot with the highest power density and a distance L to which an electron beam is collected, where a formula combining V_a , I_f^0 and L will be obtained. Then we proceed to coupon analysis.

Focusing effect of focus current

Fig. 1 show the logarithm of work distance $\log_{10}(L/\text{mm})$ as a function of the logarithm of just focus current $\log_{10}(I_f^0/\text{mA})$, where circles, triangles, squares and crosses correspond to data from the experiment for $V_a = 150 \text{ kV}$, 120 kV , 90 kV and 60 kV , respectively. Black line, black dotted line, gray line and gray dotted line are regression lines of corresponding data. A beam current is fixed at $I_b = 2 \text{ mA}$. As is shown in Fig. 1, $\log_{10}(L/\text{mm})$ is proportional to $\log_{10}(I_f^0/\text{mA})$, where the average slope of these four lines is given by -8 . Thus we obtain

$$\log_{10}\left(\frac{L}{\text{mm}}\right) = -8 \log_{10}\left(\frac{I_f^0}{\text{mA}}\right) + \dots \quad (1)$$

Fig. 2 show the logarithm of just focus current $\log_{10}(I_f^0/\text{mA})$ as a function of the logarithm of accelerating voltage $\log_{10}(V_a/\text{kV})$, where filled circles, open circles, filled triangles, open triangles, filled squares and open squares correspond to data from the experiment for $L = 700 \text{ mm}$, 600 mm , 500 mm , 400 mm , 300 mm and 200 mm , respectively. Black line, gray line, black dotted line, gray dotted line, black dashed line and gray dashed line are regression lines of corresponding data. A beam current is fixed at $I_b = 2 \text{ mA}$. As is the case with Fig. 1, using the average slope of these lines 0.5 , we obtain

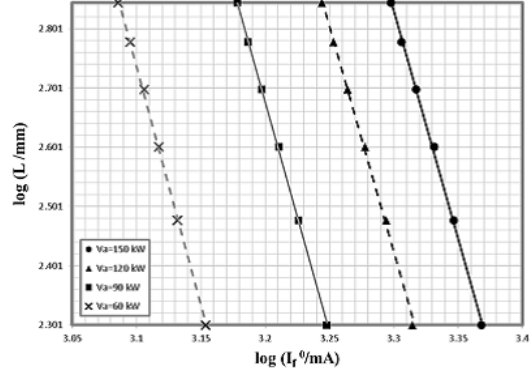


Figure 1: The logarithm of work distance $\log_{10}(L/\text{mm})$ as a function of the logarithm of just focus current $\log_{10}(I_f^0/\text{mA})$. Circles, triangles, squares and crosses are data from the experiment for $V_a = 150 \text{ kV}$, 120 kV , 90 kV and 60 kV , respectively. Black line, black dotted line, gray line and gray dotted line are regression lines of corresponding data. A beam current is fixed at $I_b = 2 \text{ mA}$.

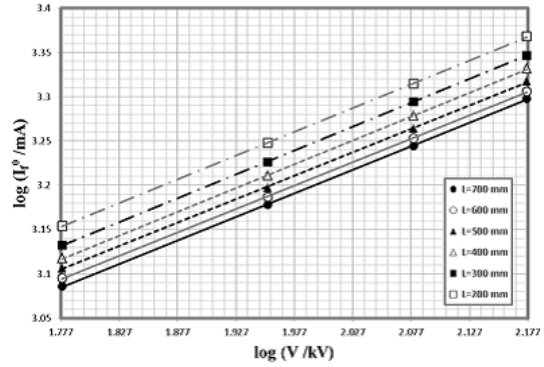


Figure 2: The logarithm of just focus current $\log_{10}(I_f^0/\text{mA})$ as a function of the logarithm of accelerating voltage $\log_{10}(V_a/\text{kV})$. Filled circles, open circle, filled triangles, open triangles, filled squares and open squares correspond to data from the experiment for $L = 700 \text{ mm}$, 600 mm , 500 mm , 400 mm , 300 mm and 200 mm , respectively. Black line, gray line, black dotted line, gray dotted line, black dashed line and gray dashed line are regression lines of corresponding data. A beam current is fixed at $I_b = 2 \text{ mA}$.

open squares correspond to data from the experiment for $L = 700 \text{ mm}$, 600 mm , 500 mm , 400 mm , 300 mm and 200 mm , respectively. Black line, gray line, black dotted line, gray dotted line, black dashed line and gray dashed line are regression lines of corresponding data. A beam current is fixed at $I_b = 2 \text{ mA}$. As is the case with Fig. 1, using the average slope of these lines 0.5 , we obtain

$$\log_{10}\left(\frac{I_f^0}{\text{mA}}\right) = 0.5 \log_{10}\left(\frac{V_a}{\text{kV}}\right) + \dots \quad (2)$$

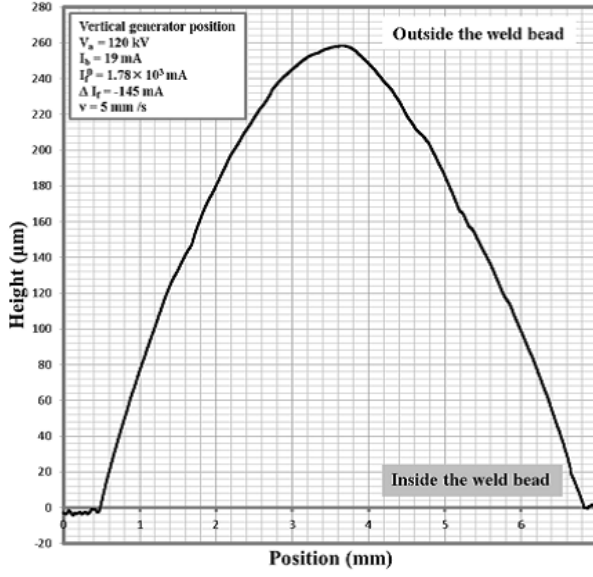


Figure 3: A typical profile of underbead for the vertical generator position. Accelerating voltage, beam current, focus current and sweep speed are 120 kV, 19 mA, $I_f = I_f^0 + \Delta I_f$ ($I_f^0 = 1.78 \times 10^3$ mA, $\Delta I_f = -145$ mA) and 5 mm/s, respectively.

To proceed, we assume a relation $L \propto V_a^\alpha I_f^{0\beta}$, namely,

$$\log_{10}\left(\frac{L}{\text{mm}}\right) = \alpha \log_{10}\left(\frac{V_a}{\text{kV}}\right) + \beta \log_{10}\left(\frac{I_f^0}{\text{mA}}\right) + \dots, \quad (3)$$

where α and β are positive or negative real. Comparing Eq.(1) and (3), and comparing Eq.(2) and (3), we find $\beta = -8$ and $-\alpha/\beta = 0.5$, namely, $\alpha = 4$. Thus we obtain

$$L \propto \frac{V_a^4}{I_f^{08}}. \quad (4)$$

From Eq.(4), we can construct a convenient parameter which represent focusing effect of a focus current. Supposing that a distance to which an electron beam is collected is shifted by ΔL when a focus current is shifted from I_f^0 by ΔI_f , we obtain

$$\Delta L = L(I_f^0 + \Delta I_f) - L(I_f^0) \propto -\frac{V_a^4}{I_f^{08}} \frac{\Delta I_f}{I_f^0}, \quad (5)$$

where $(\Delta I_f/I_f^0)^2$ is neglected. Thus a distance to which an electron beam is collected is shifted by a quantity proportional to

$$D \equiv -\frac{V_a^4}{I_f^{08}} \frac{\Delta I_f}{I_f^0}. \quad (6)$$

In the following, we call D a defocus parameter and ΔI_f a defocus current. Eq.(6) will be used for analysing coupon in the following.

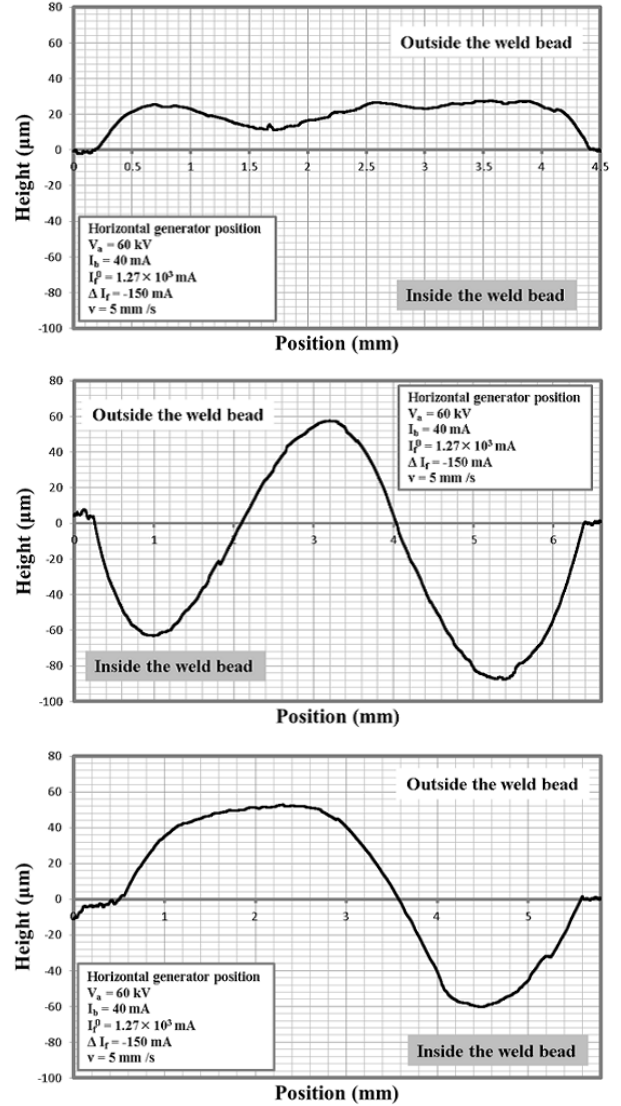


Figure 4: Typical profiles of underbeads for the horizontal generator position. The top figure is for the case that a beam sweeps from top to bottom and forms a bead vertical to the ground. The middle figure is for the case that a beam sweeps from bottom to top and forms a bead vertical to the ground. The bottom figure is for the case that a beam sweeps horizontally and forms a bead horizontal to the ground. Accelerating voltage, beam current, focus current and sweep speed are common in three and are $V_a = 60$ kV, $I_b = 40$ mA, $I_f = I_f^0 + \Delta I_f$ ($I_f^0 = 1.27 \times 10^3$ mA, $\Delta I_f = -150$ mA) and $v = 5$ mm/s, respectively.

Profile of weld beads

Before entering a quantitative analysis of bead geometry, we show rather impressive results about a relation between a profile of underbead and a beam sweep direction.

Fig. 3 shows a typical profile of underbead for the vertical generator position, where accelerating voltage, beam current, focus current and sweep speed are 120 kV, 19 mA, $I_f = I_f^0 + \Delta I_f$ ($I_f^0 = 1.78 \times 10^3$ mA, $\Delta I_f = -145$ mA)

and 5 mm/s, respectively. Fig. 4 shows typical profiles of underbeads for the horizontal generator position. The top figure is for the case that a beam sweeps from top to bottom and forms a bead vertical to the ground. The middle figure is for the case that a beam sweeps from bottom to top and forms a bead vertical to the ground. The bottom figure is for the case that a beam sweeps horizontally and forms a bead horizontal to the ground. Accelerating voltage, beam current, focus current and sweep speed are common in three and are $V_a = 60$ kV, $I_b = 40$ mA, $I_f = I_f^0 + \Delta I_f$ ($I_f^0 = 1.27 \times 10^3$ mA, $\Delta I_f = -150$ mA) and $v = 5$ mm/s, respectively. As seen in the above figures, a geometry differs from figure to figure. Fig. 3 has its peak at the center of the bead, the top figure in Fig. 4 shows a trapezoidal profile, the middle figure in Fig. 4 has its peak at the center of the bead and valleys on both sides, and the bottom figure in Fig. 4 has its peak at the down side of the bead and has a valley at the upside of the bead.

Fig. 3 can be interpreted as follows. Since a Nb coupon is horizontal, molten Nb gravitate toward a vertical to the coupon, namely the upside of the figure. As a result, a bead with a peak at the center is formed. The bottom figure in Fig. 4 can also be interpreted in much the same way. Since a Nb coupon is vertical and a formed bead is horizontal, molten Nb gravitate parallel to the coupon and vertical to the bead, namely the left-hand side of the figure. As a result, the downside of the bead (the left-hand side of the figure) swells. Although the top and middle figure in Fig. 4 is difficult to interpret, it is also thought to be due to the direction of the gravitation. Since, for the case of the top figure, a beam sweeps from top to bottom on a coupon, a direction to which molten Nb gravitate corresponds to the beam sweep direction and just below the molten Nb is molten Nb under melted at that very moment. Thus the molten Nb can not be solidified immediately. As a result, the flat surface shown in the figure is thought to be formed. On the other hand, for the case of the middle figure, a beam sweeps from bottom to top on a coupon. Since just below the molten Nb is solidifying Nb, the molten Nb is cooled rapidly than that of the top figure. This difference is thought to be a reason to form different geometry from the top figure.

Because we have enough data about the type of Fig. 3 and the bottom figure in Fig. 4, in the following, we focus attention on these kind of beads.

Allowed region of parameter space

Since we are only interested in a parameter region leading to smooth underbead, a parameter region we analyse quantitatively is limited to a region where a full penetration weld is formed without hole or weld spatter. Fig. 5 shows an example of such a parameter region, where an accelerating voltage and a sweep speed are fixed at $V_a = 60$ kV and $v = 5$ mm/s, and the generator position is fixed vertical. The horizontal axis and the vertical axis represents a beam current I_b and a defocus current ΔI_f , respectively. A circle corresponds to a full penetration weld without hole or spattering. A triangle corresponds to a partial penetration

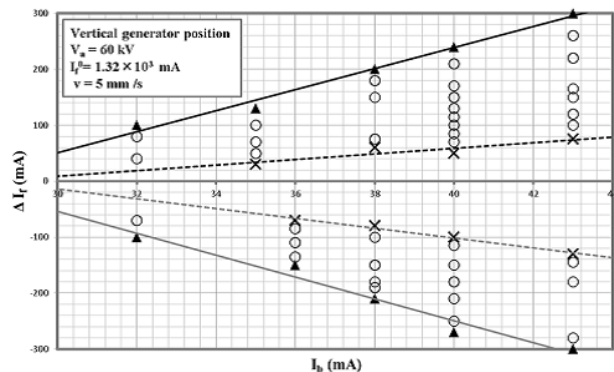


Figure 5: An example of allowed parameter region where a full penetration weld is formed without hole or weld spatter. Accelerating voltage, sweep speed and the generator position are fixed at $V_a = 60$ kV, $v = 5$ mm/s and vertical position, respectively. The horizontal axis and the vertical axis represents a beam current I_b and a defocus current ΔI_f , respectively. A circle corresponds to a full penetration weld without hole or spattering. A triangle corresponds to a partial penetration or a full penetration weld with a thin under bead. A cross means an existence of hole or weld spatter.

or a full penetration weld with a thin under bead, where a thin under bead is defined by an under bead whose width is 2 mm smaller than upper bead width. A cross means an existence of hole or weld spatter. Black line and black dotted line is a regression line for triangle and cross on $\Delta I_f > 0$ plane (upper focus region), and gray line and gray dotted line is for triangle and cross on $\Delta I_f < 0$ plane (lower focus region), which are lined for estimating boundary of allowed region.

As seen in Fig. 5, a narrow parameter region is available for a smaller beam current than that of a larger beam current. This can be easily understood as follows. For a small beam current, a sharply focused beam is needed to obtain a full penetration weld and only a small region around $\Delta I_f = 0$ is allowed. On the other hand, for a large beam current, even a defocused beam gives a full penetration bead and a large range of ΔI_f becomes allowed. This discussion is not limited to Fig. 5. A similar plot for different values of V_a or generator position also indicate a similar tendency.

Underbead width and defocus parameter

Now we confine ourselves to a parameter region where full penetration welds are formed without hole or weld spatter. First let us examine a relation between underbead widths and EBW parameters. In the following we fix a beam sweep speed at $v = 5$ mm/s and distance L at $L = 500$ mm. Thus our EBW parameters consist of an accelerating voltage V_a , a beam current I_b , a defocus current ΔI_f and a generator position. These parameters are all expected to affect under bead width.

Fig. 6 shows underbead width as a function of input

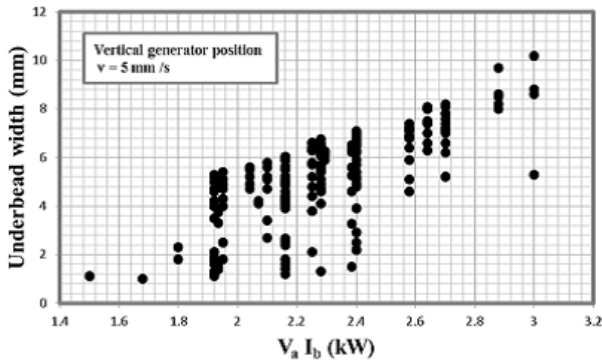


Figure 6: Underbead width as a function of input beam power. A generator position is vertical and a sweep speed is fixed at $v = 5$ mm/s.

beam power $V_a I_b$, where the generator position is vertical and sweep speed is fixed at $v = 5$ mm/s. For a specific $V_a I_b$, different values of width exist. These variations are due to different values of defocus current ΔI_f . Thus, as is expected, underbead width can not be determined uniquely by only an input beam power even for the case that v , L and generator position are fixed. A similar plot for horizontal generator position also indicate a similar tendency. In the following, we show defocusing cause different values of underbead widths for fixed beam power from a different view point.

The defocus parameter D defined by Eq.(6) is convenient in order to examine a correlation between width and input power which consist of various combinations of V_a and I_b , because the defocus parameter D can be used as a barometer for defocusing effect of ΔI_f among different V_a . Fig. 7 shows an underbead width as a function of defocus parameter. The top figure is for the vertical generator position and the bottom figure is for the horizontal generator position with the horizontal beam sweep direction. Filled circles, open circles and rhombuses represent underbead widths of vertical (horizontal) generator position for an input power of 2.58 kW(2.52 kW), 2.28 kW(2.28 kW) and 2.18 kW(2.18 kW), respectively. Note here that the right-hand side and the left-hand side of the figure corresponds to lower focus region and upper focus region, respectively, because a positive and a negative value of defocus parameter is from $\Delta I_f < 0$ and $\Delta I_f > 0$ by definition.

As seen in Fig. 7, a large beam power tends to cause a wide underbead width as is expected, and an underbead width increases as $|D|$ decreases, in other words, a focused beam cause a wide underbead. This is a natural result because defocusing affect an energy intensity on the beam spot and resultant quantity of molten Nb. A similar plot for other parameters which characterise a geometry of weld bead examined in the next subsection also indicate a similar tendency.

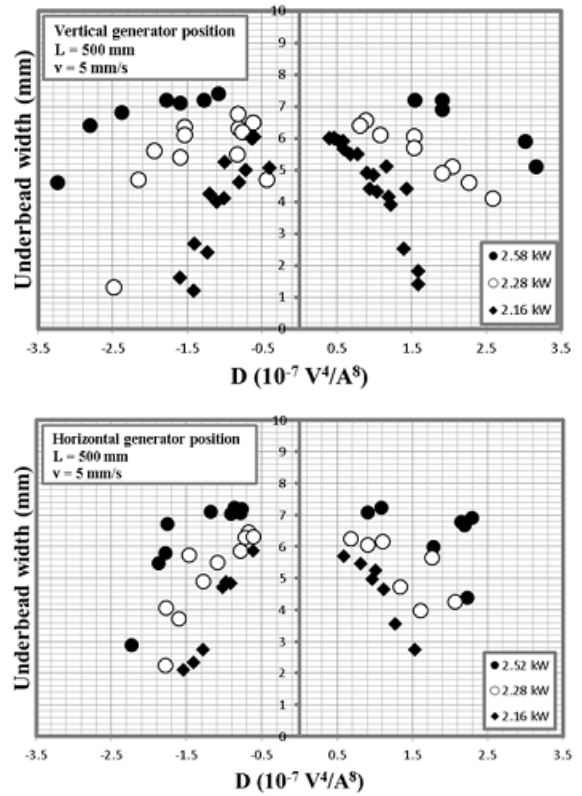


Figure 7: Underbead width as a function of defocus parameter. The top figure is for the vertical generator position and the bottom figure is for the horizontal generator position with the horizontal beam sweep direction. Filled circles, open circles and rhombuses represent underbead widths of vertical (horizontal) generator position for an input power of 2.58 kW(2.52 kW), 2.28 kW(2.28 kW) and 2.18 kW(2.18 kW), respectively.

Peak height and valley depth

Another important parameter which characterise a geometry of underbead for the vertical generator position is a peak height. Fig. 8 shows a relation between peak height of underbead and underbead width for the vertical generator position, where none of the EBW parameters are fixed except for a generator position being fixed vertical. As seen in Fig. 8, a peak height is proportional to underbead width. Therefore, the relation between peak height and defocus parameters is similar to that of width and defocus parameter because of the linearity of a peak height as a function of underbead width. Note here that the Fig. 8 itself is also useful. By using this figure, we can guess a peak height if we know an underbead width which is easier to measure.

For the horizontal generator position with the horizontal beam sweep direction, important parameter which characterise a geometry of underbead is not only a peak height and a width but also a valley depth. Fig. 9 shows a relation among peak height, valley depth and underbead width, where none of the EBW parameters except for a generator position are fixed. As seen in Fig. 9, neither a peak height

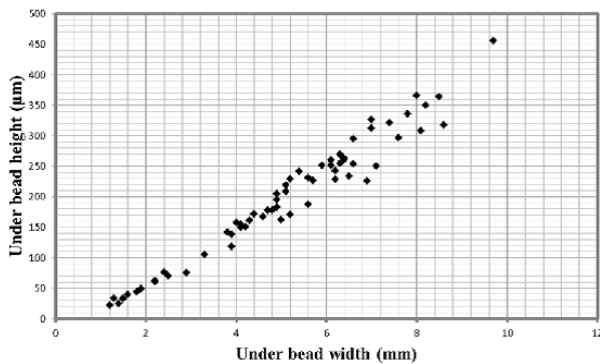


Figure 8: A relation between peak height and underbead width for the vertical generator position. None of the EBW parameters are fixed except for a generator position being fixed vertical.

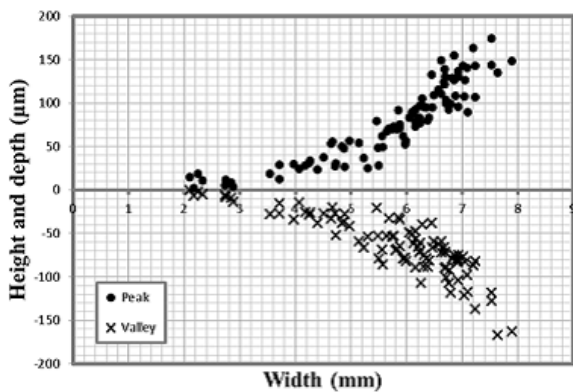


Figure 9: A relation among peak height, valley depth and underbead width for the horizontal generator position with a horizontal direction of beam sweep. None of the EBW parameters are fixed except for a generator position being fixed horizontal.

nor valley depth shows a simple linearity as a function of underbead width unlike the case for the vertical generator position. Both a peak height and valley depth increase at an accelerated pace with increasing width. Therefore, the relation between peak height or valley depth and defocus parameter is similar to that of width and defocus parameter except for their slopes being rapid because of the non-linearity of a peak height and a valley depth as a function of underbead width.

The origine of a different behavior between Fig. 8 and Fig. 9 is thought to be related to the direction of gravitation, but the detailed explanation remains to be seen.

CONCLUSION

We studied relations between electron beam welding parameters and appearances of weld beads. For the vertical generator position and the horizontal generator position with horizontal beam sweep, allowed parameter regions to obtain a full penetration weld without hole or spattering are surveyed. In addition, we examined a relation between un-

derbead width and EBW parameters by using the defocus parameter we defined. A relation between a peak height and underbead width for the vertical generator position, and a relation among a peak height, valley depth and underbead width for the horizontal generator position with horizontal beam sweep were also examined. We found that a beam generator direction and beam sweep direction affect a geometry of weld bead dramatically, a focused beam cause a wide underbead, a peak height is proportional to underbead width for the vertical generator position, and neither a peak height nor valley depth shows a simple linearity as a function of underbead width for the horizontal generator position with horizontal beam sweep.

ACKNOWLEDGMENT

We would like to thank KEK CFF group for valuable discussions and their encouragement.

REFERENCES

- [1] H. Padamsee, J. Knobloch, and T. Hays, RF Superconductivity for Accelerators (John Wiley, New York, 1998), and references therein.
- [2] Y. Iwashita, Y. Tajima, and H. Hayano, Phys. Rev. ST Accel. Beams **11**, 093501 (2008).
- [3] K. Ueno, Proceedings of the 8th Annual Meeting of Particle Accelerator Society of Japan (August 1-3, 2011, Tsukuba, Japan), p10.
- [4] T. Saeki, Proceedings of the 8th Annual Meeting of Particle Accelerator Society of Japan (August 1-3, 2011, Tsukuba, Japan), p1255.